Available online at www.sciencedirect.com
SCIENCE DIRECT®
Journal of Chromatography A, 1028 (2004) 211–218
JOURNAL OF CHROMATOGRAPHY A
www.elsevier.com/locate/chroma

Simulation of size-exclusion chromatography distribution coefficients of comb-shaped molecules in spherical pores Comparison of simulation and experiment

Wolfgang Radke*

Deutsches Kunststoff-Institut (German Institute for Polymers), Schlossgartenstr 6, Darmstadt D-64289, Germany

Received 15 September 2003; received in revised form 7 November 2003; accepted 28 November 2003

Abstract

Simulations of the distribution coefficients of linear polymers and regular combs with various spacings between the arms have been performed. The distribution coefficients were plotted as a function of the number of segments in order to compare the size exclusion chromatography (SEC)-elution behavior of combs relative to linear molecules. By comparing the simulated SEC-calibration curves it is possible to predict the elution behavior of comb-shaped polymers relative to linear ones. In order to compare the results obtained by computer simulations with experimental data, a variety of comb-shaped polymers varying in side chain length, spacing between the side chains and molecular weights of the backbone were analyzed by SEC with light-scattering detection. It was found that the computer simulations could predict the molecular weights of linear molecules having the same retention volume with an accuracy of about 10%, i.e. the error in the molecular weight obtained by calculating the molecular weight of the comb-polymer based on a calibration curve constructed using linear standards and the results of the computer simulations are of the same magnitude as the experimental error of absolute molecular weight determination.

Keywords: Simulations; Distribution coefficients; Comb-polymers; Polymers

1. Introduction

Size exclusion chromatography (SEC) has become a major tool for polymer characterization. The calibration curve needed for the evaluation of unknown substances is easily constructed by plotting the logarithm of molecular weight versus elution volume. For branched polymers, however, the situation is more complicated. Branched polymers exhibit a more dense structure than their linear analogues [1]. As a result the molecular weights obtained for branched polymers resulting from the use of a calibration curve based on linear standards are lower than the true molecular weights. This problem can be overcome by using molecular weight sensitive detectors like on-line viscosity or on-line light-scattering detectors [2–6]. However, the high price of such instruments prevents the use of such instrumentation in many laboratories. Thus, it would be helpful if the elution volume of a branched polymer relative to the linear molecule could be predicted from theory or simulation.

Experimentally it is generally accepted that the factor governing elution behavior in SEC is molecular size and not molecular weight. The widely accepted concept of universal calibration [7,8] states that molecules having identical elution volumes have identical products of $M[\eta]$, where M is the molecular weight and $[\eta]$ is the intrinsic viscosity of the polymer under investigation. However, no theoretical derivation exists for a relationship of hydrodynamic volume and distribution coefficient. It is based purely on experimental results. Beside theoretical work on the distribution coefficients of simple geometric molecules in pores of simple geometries [9], some work has appeared to date investigating the elution behavior of chain molecules in SEC either theoretically or by computer simulation. A review of Teraoka summarized the early results [10].

Casassa and co-workers [11,12] calculated the distribution coefficients for linear chains and stars in spherical and cylindrical pores. His model involved Gaussian chains for the polymer molecules. For linear polymers the ratio R_g/R_p

* Fax: +49-6151-292855.
E-mail address: wradke@dki.tu-darmstadt.de (W. Radke).

0021-9673/$ – see front matter © 2004 Elsevier B.V. All rights reserved.
doi:10.1016/j.chroma.2003.11.103

determines the distribution coefficient, where R_g and R_p are the root of the mean squared radius of gyration and the pore radius, respectively. Star polymers, however, do not lie on the same R_g/R_p-curve.

Theoretical expressions for linear chain molecules covering all regions of polymer chromatography from adsorption over chromatography at the critical point of adsorption to size exclusion mode have been derived by two Russian groups [13–15]. The results on linear chains for the size exclusion mode coincide with the results of Casassa. However, to the authors knowledge no calculations have yet been published for branched structures beside the results of Casassa.

Simulations of model chains of varying flexibility were performed by Degoulet et al. [16]. They found that universal calibration is not strictly valid if the molecules differ in their flexibility. Boyd et al. [17] performed molecular dynamics simulations of polystyrene, polyethylene and polyisobutylene oligomers. They showed that these oligomers do not obey the universal calibration principle. Both studies compared linear macromolecules of different chemistry or different chain flexibility.

Bleha and co-workers [18–20] used computer simulations to investigate the effect of solvent quality on linear macromolecules confined between parallel walls. Their results indicate that the solvent quality does not alter the dependence of the partition coefficient on the ratio of mean squared radius of gyration to pore radius. Furthermore, they found increasing partition coefficients with increasing polymer concentrations. Again, only linear chains have been investigated.

Simulations on branched polymers were performed by Tobita et al. and by Jackson. Tobita and coworkers [21–24] developed an algorithm suitable to predict the different branched structures and the molecular weight distribution in a branched polymer based on the kinetic constants of the polymerization process. They were able to calculate the apparent molecular weight distribution that would result from SEC-evaluation versus a calibration curve based on linear standards. Jackson [25] performed similar simulations. Both authors calculated the mean squared radius of gyration from random walks (RW). Correction for solvent quality were done selecting an reasonable value for the parameter ε in the relationship $g' = g^{\varepsilon}$. Here, the branching ratio, g, is defined as the ratio of the mean squared radii of gyration of branched and linear molecules, having the same molecular weight. g' is the corresponding ratio of the intrinsic viscosities. The value of ε is still under dispute. It appears as if no constant value could be found to account for all experimental data of even the simplest branched molecules, the star polymers [26]. Despite this uncertainty, the simulations by Tobita and Jackson are useful to understand the effect of branching on the local polydispersity of SEC-slices and the effect of different detection systems. However, no comparison with experimental data was presented, which allows judging on how good the results of the simulations agree with experiment.

In recent publications [27,28] it has been shown that computer simulations based on self avoiding walks and a calibration curve based on linear standards can be used to predict the SEC-retention of star polymers. Furthermore, it was shown that the error in the molecular weight based on computer simulation is of the same size as the error associated with absolute methods of molecular weight characterization but lower than the error resulting from using a calibration curve constructed based on linear standards. The present paper extends this work to comb-shaped polymers as the next complicated branched species.

2. Experimental

2.1. Simulations

The simulations were performed using a program written by the author. Calculations were performed on standard personal computers. Since the properties of self avoiding walks should be investigated, the pivot algorithm was used for the creation of different molecular configurations. The properties of linear and star polymers simulated using the pivot-algorithm has been investigated in detail by Zifferer [29,30]. The first step of the algorithm used by the author consists of the creation of a non-reversal random walk (NRRW) for the particular architecture on a diamond lattice. The phantom chains consist of N mass points connected by $N-1$ bonds of length $l = \sqrt{3}$. The linear chains were created by starting the chain at the origin. The second mass point was assigned to position (1, 1, 1). The next position was selected randomly from $x_i = x_{i-1} \pm 1$, $y_i = y_{i-1} \pm 1$, $z_i = z_{i-1} \pm 1$, until the condition $|r_i - r_{i-2}| = \sqrt{8}$ was fulfilled. The branched structures (combs) were obtained by first generating a linear backbone chain of N_{bb} masspoints (backbone). The N_b arms of length N_{SC} where attached on the backbone at a regular fixed spacings of $SP = N_{bb}/(N_b + 1)$, restricting the position of the first attached side chain segments to the lattice points not occupied by neighboring mass points of the backbone.

The NRRW was allowed to relax by a random mixture of pivot and repetition trials [31] until the first SAW was obtained. The global properties of such first self avoiding walks are close to those of SAWs [31]. This SAW served as starting point for data sampling. Sampling was performed until the mean squared radius of gyration was constant within 5% over the last $3N$ conformations. Test simulations for some topologies showed, that the mean squared radius approaches a constant value slower than the hydrodynamic radius or the average distribution coefficient. When a constant value of R_g was reached, the averages for the radius of gyration, R_g, hydrodynamic radius, R_h, and distribution coefficient, K, were stored. The last conformation served as start for the next averaging procedure. Typically 100 such averages were taken for a particular topology. From these averages the errors can be estimated [29,32]. Stable R_g-values were

obtained typically after $5N$ conformations. Thus, a typical number of $500N$ conformation were used for the calculations of the final averaged properties.

Calculation of significant quantities:

The mean squared radius of gyration for a particular conformation was calculated using [33]:

$$\langle R_g^2 \rangle = \frac{\sum_{i=1}^{N} r_i^2}{N} - \frac{1}{N^2}\left(\sum_{i=1}^{N} r_i\right)^2 \quad (1)$$

where r_i denotes the vector from the first to the ith mass point of the chain. Comparison of the simulated R_g values with available literature data on linear and star-shaped polymers on tetrahedral lattices showed good agreement [29,30,33]. This indicates, the correctness of the algorithms for chain creation, relaxation and sampling as well as for the calculation of the root mean squared radius, R_g.

In the non-draining limit, the friction coefficient, Ξ, can be expressed as [34,35]:

$$\Xi = \frac{3\pi\eta_0 N^2}{\sum_i \sum_{j>i} \langle r_{ij}^{-1} \rangle} \quad (2)$$

where $\langle r_{ij}^{-1} \rangle$ denotes the average over all conformations and η_0 the viscosity of the solvent. Friction coefficient and hydrodynamic radius, R_h, are related via:

$$\langle R_h \rangle = \frac{\Xi}{6\pi\eta_0} = \frac{N^2}{2\sum_i \sum_{j>i} \langle r_{ij}^{-1} \rangle} \quad (3)$$

According to Eq. (3) the time for the simulation of R_h scales with N^2, since the average between each pair of mass points has to be calculated. In order to save computing time only an estimate for R_h was calculated. Eq. (3) involves two averages. First the average over all conformations as expressed by the brackets, second the average over all possible inter mass point distances as expressed by the double sum. Upon reversing the order of averaging, we replaced the exact average over the double sum by the average over N arbitrary inter mass point distances. Thus:

$$\frac{2\sum_i \sum_{j>i} \langle r_{ij}^{-1} \rangle}{N^2} = \left\langle \frac{2\sum_i \sum_{j>i} r_{ij}^{-1}}{N^2} \right\rangle \approx \left\langle \frac{\sum_{k=1}^{N} r_{i_k j_k}^{-1}}{N} \right\rangle \quad (4)$$

Comparing the errors associated with this procedure shows only negligible effects on the results.

The calculation of the average distribution coefficient needs to determine the average accessible fraction of the pore volume for the particular architecture. For the simulation of the distribution coefficient of a particular conformation the center of gravity, S, was placed in the center of the pore of radius R_p. An arbitrary direction was chosen, and the displacement vector, r, at which the chain intersects the wall of the sphere, was calculated. A volume $V_{dir} = 4/3\pi r^3$ was assigned to the particular direction, and the volume was averaged over D different directions. Typically a value of $D = 30$ was used. The distribution coefficient of the configuration, K_{conf}, was calculated as:

$$K_{conf} = \frac{4\pi \sum_D V_{dir}}{D 3 R_p^3} \quad (5)$$

The distribution coefficient for a defined topology was obtained by averaging over the all simulated conformations. By replacing the lattice chains by random flight chains of fixed segment length, comparison was made with theoretical results for linear chains [11]. Good agreement was found for the simulated and theoretical results obtained, indicating that the algorithm for the determination of the distribution coefficient works successfully. More detailed information on the algorithm can be found elsewhere [27].

2.2. Synthesis

Comb-shaped poly(*p*-methyl styrene)s were synthesized by grafting phenanthrene-labeled poly(*p*-methyl styrene)anions onto partially brominated linear poly(*p*-methyl styrene)s [36,37]. The incorporation of the phenanthrene group into the side chains was achieved by reacting living poly(*p*-methyl styrene)anions with 1-phenanthryl-1-phenyl-ethylene [36,38] prior to the coupling reaction. A part of the labelled polymer was withdrawn for calibration purposes (see below). The details of the synthesis will be published elsewhere [39].

2.3. Characterization

SEC-analyses were performed in THF at 0.5–1 ml/min using 5 μ PSS SDV columns (10^3, 10^5, 10^6 Å; 30 cm × 0.8 cm each). Applied Biosystems S1000 UV diode array and Bischoff 8110 RI-detector were used. A Viscotek H502 B and/or a Wyatt Technology DAWN-F multi-angle light-scattering detector could be added. However, for the present investigation only light-scattering data were used. Data acquisition was performed using PSS WinGPC and Wyatt Technology Winastra software. The injected amounts and flow rates were adjusted depending on molecular weights and polydispersities of the samples.

For conventional SEC-experiments toluene was used as an internal flow marker, to correct for flow rate fluctuations. SEC-calibrations were performed using a series of poly(*p*-methyl styrene)s with narrow and broad distributions which have been synthesized by the author. The samples where analyzed by SEC-light scattering. For two samples the results obtained were independently crosschecked by conventional static light-scattering measurements. Weight average molecular weights found by this independent analysis were in good agreement.

The light-scattering instrument was calibrated using pure toluene assuming Rayleigh ratio of $9.78 \times 10^{-6}\,cm^{-1}$ at 633 nm. The exact injection volume of the fixed autosampler loop was determined gravimetrically by filling the loop repeatedly with distilled water. The refractive index

increments of poly(*p*-methyl styrene) was estimated from the response of the RI-detector. In order to do so, the detector response was calibrated using polystyrene standards and assuming a d*n*/d*c* value of 0.189 cm^3/g. Assuming the dispersions of polystyrene and poly(*p*-methyl styrene) to be very similar, an average value of $dn/dc = 0.170\ cm^3/g$ was found from the relative responses. However, since the refractometer uses a different wavelength than the light-scattering instrument, the d*n*/d*c* value was crosschecked for three samples using a scanning interferometer operated at a wavelength of 633 nm. This determination results in an average of $dn/dc = 0.177\ cm^3/g$, which is in good agreement with the value found from the refractive index detector.

Determination of the composition of the comb-polymers was performed for the individual slices in the following way. After suitable calibration of the detector responses for the labeled and non-labeled poly(*p*-methyl styrene)s, the composition was calculated assuming additivity of the responses of the individual components.

3. Results and discussion

3.1. Simulation

The simulations were performed for linear and comb-polymers in pores of radius 75 and 150 units. Thus, the sphere radii were taken to be 43.3 and 86.6 times the length of a repeating unit. Fig. 1 shows the calibration curves of linear and comb-shaped polymers having 50 wt.% of side chains. We can see that the calibration curves for the larger pore size is more suited for the separation of higher molecular weight samples. The separation region of a single pore size covers roughly 1.5–2 orders of molecular weight. This is in agreement with columns selection charts of typical individual pore size columns. Comb-shaped molecules elute later than linear molecules of the same molecular weight. That is at a particular elution volume the molecular weight of the branched molecule is higher than that of the linear molecule, indicating the higher segment density of the branched species. The difference of the calibration curves for linear and comb-shaped is molecular weight dependent. For low molecular weights, i.e. small number of branch points, the deviation is weak but increases with increasing molecular weight until a nearly constant distance between the calibration curves is obtained. Thus, for sufficiently high number of branches a constant factor should describe the deviation between the calibration curves of linear and comb-shaped polymers.

Fig. 2 compares the calibration curves for different weight fractions of side chains in a pore of size $R_p = 75$. The deviation between the calibration curve for the linear polymer and the comb-shaped polymer increases with increasing weight fraction of side chains.

According to SEC-theory, the key parameter determining the elution behavior is not the molecular weight but the molecular size in solution. A convenient way to characterize the size of a molecule in solution is the use of its mean squared radius of gyration. This parameter can be determined by static light-scattering experiments. It is also easily accessible by calculation. Fig. 3 shows $\langle R_g^2 \rangle^{1/2}$ as a function of the distribution coefficient. It can be seen that the correlation is slightly better than using the molecular weight.

Significant improvement is however made, when the distribution coefficient is plotted versus the hydrodynamic radius, R_h (Fig. 4). Irrespective of the particular architecture, all data points fall onto a common curve. It therefore appears as if the hydrodynamic radius can be used to describe the elution behavior. If this is the case, a normalized plot of R_h/R_p versus distribution coefficient should result in a single curve independent of architecture and pore size. Fig. 5 shows that this criterion is well fulfilled for the combs investigated.

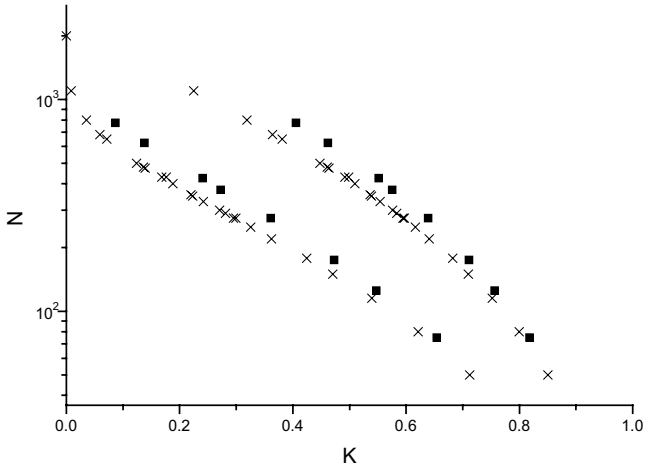

Fig. 1. Calibration curves for linear (×) and comb-shaped polymers ($N_{SC} = 25$, SP = 25, $w_{SC} = 0.5$, ■) in spherical pores of pore radius $R_p = 75$ (lower curves) and 150 (upper curves), respectively.

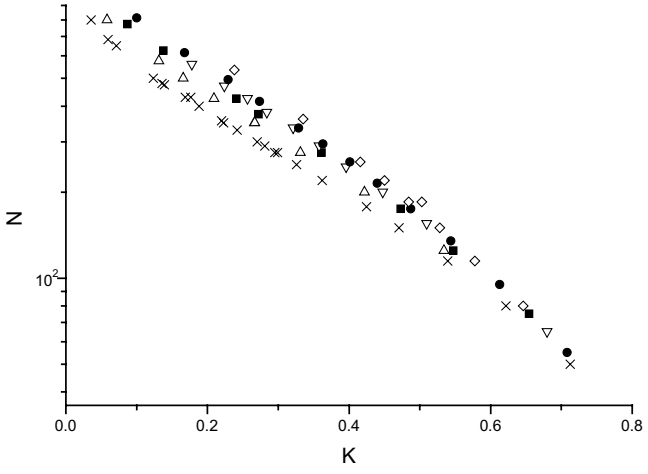

Fig. 2. Calibration curves for linear (×) and comb-shaped polymers ($N_{SC} = 25$, $w_{SC} = 0.33$ △, 0.5 ■, 0.56 ▽, 0.62 ●, 0.71 ◇) in spherical pores of pore radius $R_p = 75$.

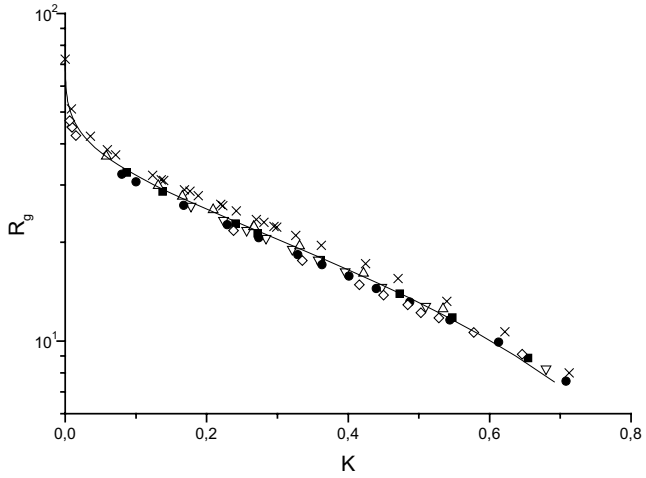

Fig. 3. Distribution coefficient as function of the root mean squared radius of gyration (R_g) for linear (×) and comb-shaped polymers ($N_{SC} = 25$, $w_{SC} = 0.33$ △, 0.5 ■, 0.56 ▽, 0.62 ●, 0.71 ◇) in spherical pores of pore radius $R_p = 75$. The solid line corresponds to the results of Casassa on linear chains in spherical pores [11].

Only for R_h/R_p-ratios less than 0.1 slight deviations occur. This observation is in agreement with the results of similar simulations on star-shaped polymers [27]. There are two possible explanations for this behavior. First, if the degree of polymerization is low, the calculation of the hydrodynamic radius might not be adequate since the corresponding equations are based on Gaussian subchains. A different explanation is the following: when comparing different pore sizes at the same hydrodynamic volume, we change the ratio of segment length to pore radius R_p. Therefore, the deviations might be explained by different degrees of chain stiffness. However, if we compare only branched and linear molecules at the same pore size, we obtain a common curve since we are comparing molecules having the same degree of stiffness.

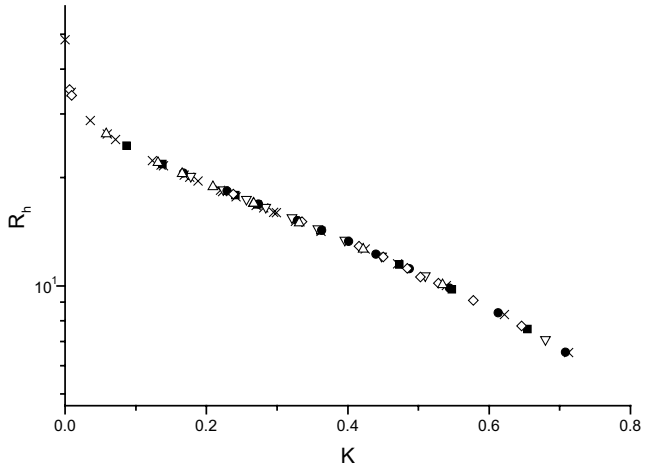

Fig. 4. Distribution coefficient as function of the hydrodynamic radius (R_h) for linear (×) and comb-shaped polymers ($N_{SC} = 25$, $w_{SC} = 0.33$ △, 0.5 ■, 0.56 ▽, 0.62 ●, 0.71 ◇) in spherical pores of pore radius $R_p = 75$.

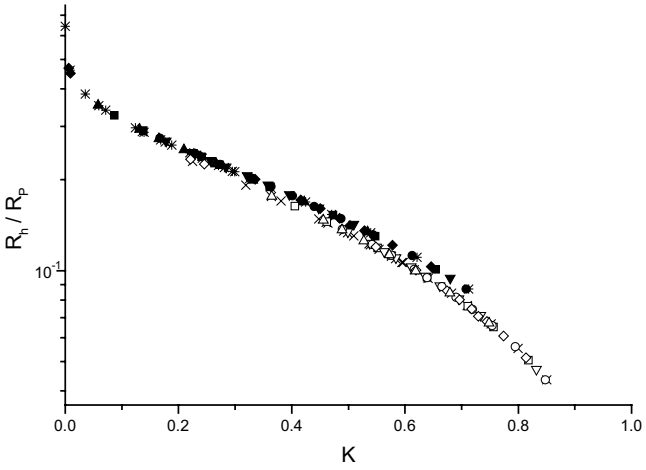

Fig. 5. Distribution coefficient as function of the ratio R_h/R_p for two different pore sizes. Linear (×, ✱) and comb-shaped polymers ($N_{SC} = 25$, $w_{SC} = 0.33$ ▲△, 0.5 □■, 0.56 ▽▼, 0.62 ○●, 0.71 ◆◇). Open symbols: $R_p = 150$, solid symbols: $R_p = 75$.

By comparing the calibration curves (Figs. 1 and 2), we were able to obtain the molecular weight of a linear chain having the same distribution coefficient as a comb. That is we can compare the molecular weights of linear and branched species at identical elution volumes.

The ratio $\gamma_{sim.} = N_{branched}/N_{lin.}$ can be defined as the ratio of the molecular weights of branched and linear species having identical distribution coefficient, thus identical elution volume. These values are nearly independent of pore size (Fig. 6). They depend on the number of side chains but reached limiting values for a high number of side chains. In order to check that the obtained γ-ratios are independent of the particular length of the side chain, we performed simulations for polymers having the same weight fraction of side chains but differing in side chain length (Fig. 7). It can be seen that the ratios are independent of the particular side

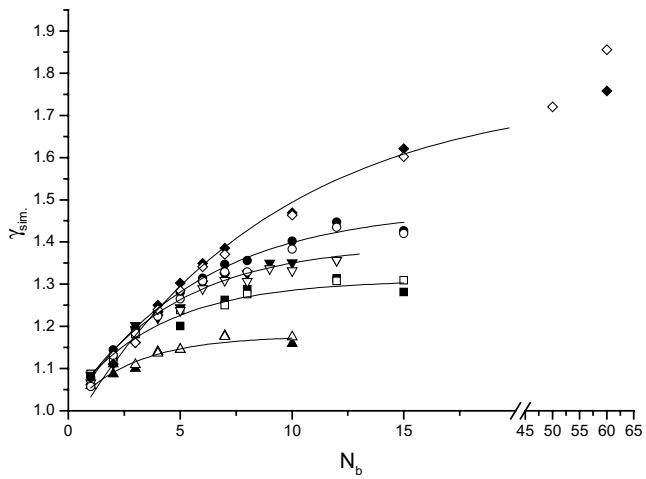

Fig. 6. Dependence of γ-ratios of comb-shaped polymers on the number of side chains, N_b ($N_{SC} = 25$, $w_{SC} = 0.33$ ▲△, 0.5 □■, 0.56 ▽▼, 0.62 ○●, 0.71 ◆◇). Open symbols: $R_p = 150$, solid symbols: $R_p = 75$.

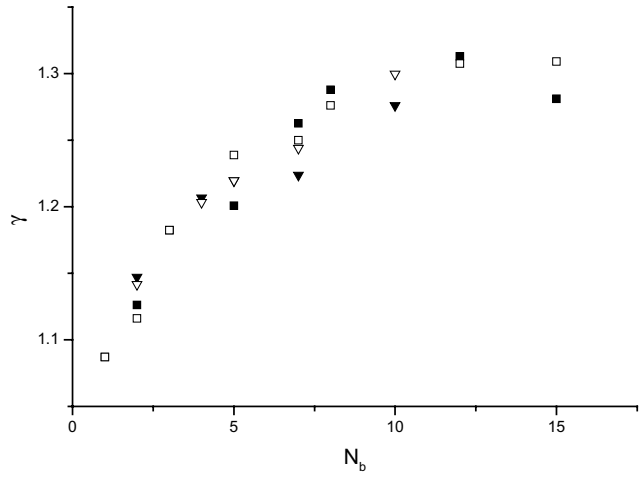

Fig. 7. Comparison of γ-ratios of comb-shaped polymers having different numbers, N_b and lengths of side chains, N_{SC} for a constant weight fraction of side chains $w_{SC} = 0.5$, □■: $N_{SC} = 25$, ▽▼: $N_{SC} = 50$). Open symbols: $R_p = 150$, solid symbols: $R_p = 75$.

chain length. Thus, it seems that for comb-polymers having a large number of side chains the error associated with the use of a linear calibration curve is only a function of the weight fraction of side chains. The dependence is shown in Fig. 8. For weight fractions below approximately 0.5 there is a nearly linear correlation between w_{SC} and $\gamma_{sim.}$. The error associated with the use of a linear calibration curve will not exceed 30%. However, for combs having higher weight fractions of side chains, a strong increase of $\gamma_{sim.}$ can be observed. Thus, for larger fractions of side chains the error associated with the use of a linear calibration curve should increase rapidly.

In a similar simulation on star-shaped polymers it was found that the effect of the excluded volume on the γ-ratios is negligible [27]. In order to verify whether this is also true for comb-shaped polymers, the simulations were also performed for non-reversal random walks, allowing for multiple occupation of lattice points. For comparison with the data obtained under good solvent conditions (SAWs), the resulting γ-values are also shown in Fig. 8. There is a substantial difference between the data sets. The NRRW-data are higher than the ones resulting from the simulations under good solvent conditions.

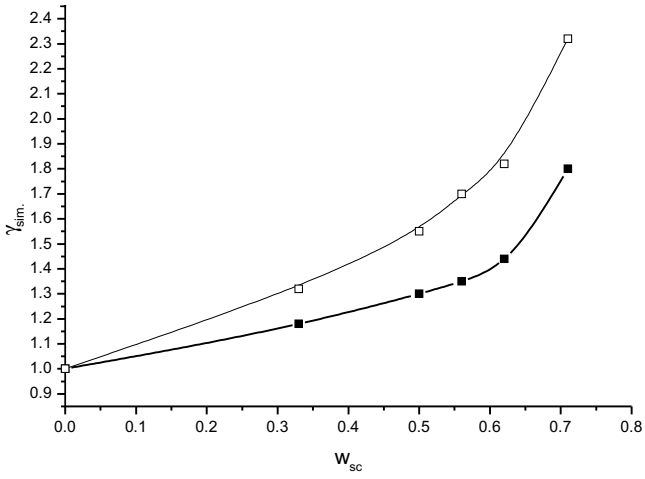

Fig. 8. Dependence of γ on weight fraction of side chains, w_{SC}, solid symbols: SAWs (good solvent), open symbols: NRRWs (Gaussian chains).

The tendency to lower γ-values under good solvent conditions can be explained by the enhanced segment density of the comb-polymer relative to the linear one. Starting from the dimension of the comb obtained from the NRRW the comb is expanded due to the excluded volume effect. As a result, the distribution coefficient for the SAW is lower than that of the NRRW. The same holds true for the linear polymer. Since a linear NRRW coeluting with the corresponding NRRW-comb has a lower molecular weight, the segment density of the comb is higher and the expansion of the linear polymer due to excluded volume effects is expected to be less than for the comb. Consequently, the reduction of the distribution coefficient due to an increase in solvent quality will be less for the linear than for the comb-polymer. The comb will coelute under good solvent conditions with a linear polymer having a higher molecular weight than under poor solvent conditions. Thus, γ_{SAW} is lower than γ_{NRRW}. The larger extention for the branched molecule relative to the linear one due to good solvents should also be valid for star shaped molecules. This, however, is not the case even for arm numbers far away from the hard sphere limit [27]. On the other hand, the results on the simulated γ-values do agree with simulations and experimental data on branching ratios g for combs and stars, where combs are found to have larger g-values than predicted from Gaussian behavior [40,41], while for stars a good agreement is found for the Gaussian model and g-values in good solvents [30].

3.2. Comparison of simulation and experiment

In order to investigate whether it is possible to predict the retention behavior of comb-polymers from computer simulations, a number of comb-polymers were characterized by SEC and SEC light-scattering experiments. Some of the combs were obtained by grafting side chains with narrow distribution onto a backbone with narrow distribution. Another series was obtained in a similar way but using a broad distributed backbone. The characterization data of the side chains and the parent backbone polymer are given in Table 1. Typical SEC-chromatograms of comb-polymers are shown in Fig. 9. It can be seen that at the low molecular weight end of the chromatogram significant amounts of non-reacted side-chains remained due to side reactions. Due to the different molecular weight dependences of the detector responses, the peak maxima of the light-scattering trace for the comb with broad distribution is shifted to higher molecular weights as compared to the RI-trace. This effect is not visible for narrow distributed comb-polymers, indicating that the peak

Table 1
Molecular characteristics the precursor polymers (backbone and grafted side)

Comb part	M_n ($\times 10^3$ g/mole)	M_w ($\times 10^3$ g/mole)	$D = M_w/M_n$
Backbone	334	910	2.72
Backbone	150	156	1.04
Side chain	3.5	3.7	1.07
Side chain	11.0	11.3	1.04
Side chain	15.4	16.0	1.04

M_w as determined by SEC/LS. M_n determined from conventional poly(*p*-methyl styrene) calibration curve.

width seems to be dominated by band broadening and only to a minor extend by polydispersity.

The characteristics of the comb-polymers are given in Table 2. The true molecular weights obtained by SEC-light scattering and the apparent molecular weights, derived from using a calibration curve based on linear poly(*p*-methyl styrene)s were taken at the maximum of the RI-trace. The composition at peak maximum was obtained from a combined UV/RI-analysis and was found to be nearly constant across the peak. In principle, it is possible to calculate composition, true and apparent molecular weights and thus γ-values for each elution volume. Band broadening effects, however, resulted in a relative large scattering for the γ-values at a specified composition. Despite this, the averages across the peak correspond well with the data obtained at the peak maxima. Fig. 10 shows the experimentally determined γ-values taken at the peak maxima and as averages over the peak in comparison with the expectations of the simulations. The use of the weight or number average molecular weights is crucial, since all polymers include

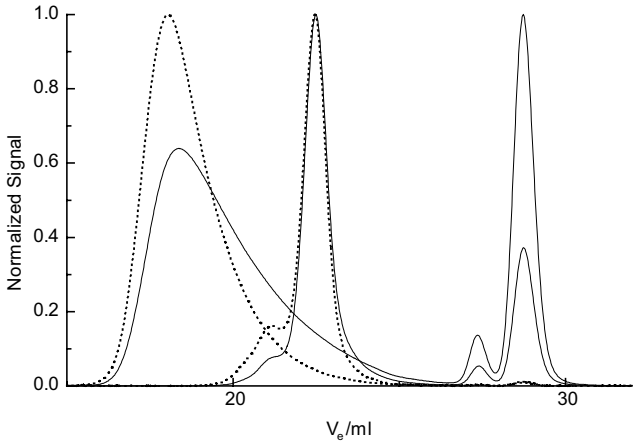

Fig. 9. SEC-chromatograms for combs obtained from backbones with narrow and broad distribution. Solid lines: RI-traces, dotted lines: 90° light-scattering traces.

Table 2
Molecular characteristics of the analyzed comb-polymers

M_w ($\times 10^3$ g/mole backbone)	M_w ($\times 10^3$ g/mole side chain)	w_{SC}[a]	$M_{w,LS}$ ($\times 10^5$ g/mole)	$D = M_{w,LS}/M_{n,LS}$	$\gamma = M_p/M_{p,app.}$
910	3.7	0.37	15.1	2.02	1.29
910	11.3	0.62	20.6	2.00	1.57
910	16.0	0.68	23.5	2.03	1.57
910	3.7	0.19	11.7	2.00	0.98
910	11.3	0.40	16.1	2.25	1.32
910	16.0	0.43	17.8	2.15	1.34
910	3.7	0.22	12.5	2.09	1.03
910	11.3	0.43	15.0	1.98	1.30
910	16.0	0.49	14.5	2.01	1.19
910	3.7	0.13	12.3	2.09	1.09
910	11.3	0.28	14.3	2.07	1.25
910	16.0	0.33	15.9	2.07	1.23
156	3.7	0.39	2.77	1.29	1.31
156	11.3	0.60	4.09	1.16	1.73
156	16.0	0.66	4.72	1.21	1.50
156	3.7	0.31	2.10	1.09	1.22
156	11.3	0.53	3.25	1.10	1.52
156	16.0	0.59	3.39	1.14	1.42
156	3.7	0.20	1.88	1.09	1.16
156	11.3	0.40	2.53	1.08	1.40
156	16.0	0.47	2.73	1.09	1.25
156	3.7	0.11	1.65	1.07	1.08
156	11.3	0.20	1.88	1.07	1.26
156	16.0	0.29	2.08	1.09	1.13

$M_{w,LS}$: obtained from SEC/LS. $M_{n,LS}$: obtained from SEC/LS.
[a] Value taken at peak maximum.

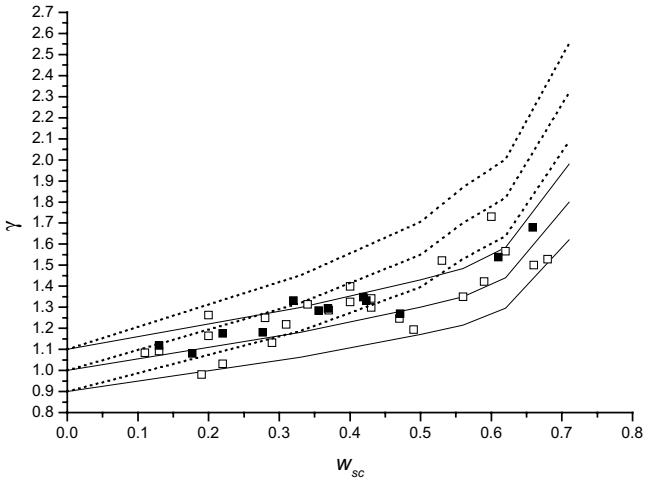

Fig. 10. Comparison of γ-values from simulation and from experiment. Solid lines correspond to the SAW-results and the ±10% deviation thereof (good solvent). Dotted lines indicate the NRRW-results (Gaussian chains) and the respective ±10% deviation. Open symbols: average taken over slices, solid symbols: data taken at peak maxima.

significant amounts of precursor molecules. Furthermore, the ratios $\bar{\gamma} = M_{\mathrm{w}}/M_{\mathrm{w,app.}}$ are difficult to interpret. Thus, for the sake of clarity only the data for the peak maxima and for the averages have been included in Fig. 10.

It becomes clear that the results from the simulations of SAWs correspond to the experimental data in contrast to the results of the RWs. Three out of four data points were found within a 10% error of the simulation. Allowing for an error of 15%, we find all experimental data points except one. Since the typical error associated with the absolute determination of a molecular weight has to be considered to be in the error of 10–15%, it is possible to conclude that the prediction of calibration curves for branched polymers by computer simulation is as accurate as the absolute determination of molecular weights. The simulations, however, have to include the effect of solvent quality. Predictions based on random walks or NRRWs might lead to significant errors due to ignoring the coil expansion in good solvents.

4. Conclusions

It was shown that it is possible to predict the retention behavior of comb-polymers based on simulations and the calibration curve of the linear polymer, provided the molecular weight are sufficiently high. For high molecular weight branched polymers computer simulations can help to obtain calibration curves for branched materials for which no standards are available. At large numbers of side chains, the deviation of the calibration curves for combs from the calibration curves of the corresponding linear polymer is only a function of the weight fraction of material in the side chains. Knowing the ratio of true and apparent molecular weight, it is possible to obtain the weight fraction of side chains.

Acknowledgements

The author thanks Mrs. Christine Rosenauer (Max Planck Institute of Polymer Science, Mainz) for performing static light-scattering measurements and for determining the refractive index increment of poly(*p*-methyl styrene).

References

[1] B.H. Zimm, W.H. Stockmayer, J. Chem. Phys. 17 (1949) 1301.
[2] M.A. Haney, J. Appl. Polym. Sci. 30 (1985) 3037.
[3] M.A. Haney, J. Appl. Polym. Sci. 30 (1985) 3023.
[4] M.A. Haney, A. Am. Lab. 17 (1985) 116.
[5] P.J. Wyatt, Anal. Chim. Acta 272 (1993) 1.
[6] W.W. Yau, Chemtracts, Macromol. Chem. 1 (1990) 1.
[7] H. Benoît, Z. Grubisic, P. Rempp, D. Decker, J.G. Zilliox, J. Chim. Phys. 63 (1966) 1507.
[8] Z. Grubisic, P. Rempp, H. Benoit, J. Polym. Sci.: Polym. Lett. 5 (1967) 753.
[9] J.C. Giddings, E. Kucera, C.P. Russell, M.N. Myers, J. Chem. Phys. 72 (1968) 4397.
[10] I. Teraoka, Prog. Polym. Sci. 21 (1996) 89.
[11] E.F. Casassa, Y. Tagami, Macromolecules 2 (1969) 14.
[12] E.F. Casassa, J. Polym. Sci. B.: Polym. Lett. 5 (1967) 773.
[13] A.A. Gorbunov, A.M. Skvortsv, Adv. Colloid Interface Sci. 62 (1995) 31.
[14] S.G. Entelis, V.V. Evreinov, A.V. Gorshkov, Adv. Polym. Sci. 76 (1986) 129.
[15] A.A. Gorbunov, L.Ya. Solovyova, V.A. PaSEChnik, J. Chromatogr. 448 (1988) 307.
[16] C. Degoulet, J.-P. Busnel, J.-F. Tassin, Polymer 35 (1994) 1957.
[17] R.H. Boyd, R.R. Chance, G. Ver Strate, Macromolecules 35 (1996) 1182.
[18] P. Cifra, T. Bleha, A. Romanov, Polymer 29 (1988) 1664.
[19] P. Cifra, T. Bleha, F.E. Karasz, Polymer 31 (1990) 1321.
[20] Y. Wang, I. Teraoka, P. Cifra, Macromolecules 34 (2001) 127.
[21] H. Tobita, S. Saito, Macromol. Theory Simul. 8 (1999) 513.
[22] H. Tobita, N. Hamashita, Macromol. Theory Simul. 9 (2000) 453.
[23] H. Tobita, N. Hamashima, J. Polym. Sci., Part B: Polym. Phys. 38 (2000) 2009.
[24] H. Tobita, H. Kawai, E-Polym. (2002) 048, http://www.e-polymers.org.
[25] C. Jackson, J. Chromatogr. A 662 (1994) 1.
[26] M.K. Mishra, S. Kobayashi S. Star, Hyperbranched Polymers, Marcel Dekker, New York, Basel, 1999, pp. 308–314.
[27] W. Radke, Macromol. Th. Simul. 10 (2001) 668.
[28] W. Radke, J. Gerber, G. Wittman, Polymer 44 (2003) 519.
[29] G. Zifferer, Macromolecules 23 (1990) 3166.
[30] G. Zifferer, Makromol. Chem. 191 (1990) 2717.
[31] G. Zifferer, Macromol. Simul. 6 (1991) 103.
[32] H. Flyvberg, H.G. Petersen, J. Chem. Phys 91 (1989) 461.
[33] L.V. Gallacher, S. Windwer, J. Chem. Phys. 44 (1966) 1139.
[34] X.F. Yuan, A.J. Masters, J. Chem. Phys. 94 (1991) 6908.
[35] W.H. Stockmeyer, M. Fixman, Ann. N.Y. Acad. Sci. 57 (1953) 334.
[36] W. Radke, Ph.D. Thesis, Johannes Gutenberg Universität, Mainz, 1996.
[37] W. Radke, A.H.E. Müller, Am. Chem. Soc., PMSE Prepr. 40 (2) (1999) 144.
[38] Z. Hruska, B. Vuillemin, G. Riess, A. Katz, M.A. Winnik, Macromol. Chem. 193 (1992) 1987.
[39] W. Radke, A.H.E. Müller, in preparation.
[40] J.E.G. Lipson, Macromolecules 24 (1991) 1327.
[41] J.E.G. Lipson, Macromolecules 26 (1993) 203.